ORIGINAL RESEARCH

An Ex Vivo Study of Filum Terminale in Children and Fetuses Based on Optical Coherence Tomography

Weidong Jia, Mmed; Liangkui Wei, Mmed; Jianfeng Li, Mmed; Bing Xia, PhD; Xianxu Zeng, PhD; Weiming Hu, Mmed; Yu Zhang, Mmed; Fuyun Liu, PhD

ABSTRACT

Objective • To distinguish *ex vivo* normal and abnormal filum terminale (FT) in pathology based on optical coherence tomography (OCT).

Methods • A total of 14 *ex vivo* FTs, freshly imaged via OCT after being cut, were excised from the scanned region for histopathological examination (HPE). Qualitative analysis was performed by 2 blinded assessors.

Results • We performed OCT imaging of all specimens and validated them qualitatively. In the fetal FTs, we observed large amounts of fibrous tissue scattered throughout with a few capillaries but no adipose tissue. In tight filum terminale syndrome (TFTS), adipose infiltration and capillaries were significantly increased, with obvious fibroplasia and disarrangement. OCT images showed increased adipose tissue in which the adipocytes were arranged in a grid-like pattern; dense, disordered fibrous tissue and vascular-like tissue were present. The diagnostic results of OCT and HPE were consistent (Kappa = 0.659; $P = .009, <.01$), and there was no statistically significant difference in diagnosing TFTS using a Chi-square test ($P > .05$). The area under the curve (AUC) for OCT (AUC = 0.966; 95% CI, 0.903 to 1.000) was better than magnetic resonance imaging (MRI) (AUC = 0.649; 95% CI, 0.403 to 0.896).

Conclusion • OCT can quickly obtain clear images of FT's inner structure, contribute to diagnosing TFTS and will be an indispensable complement to MRI and HPE. More FT sample studies *in vivo* are needed to confirm the high accuracy rate of OCT (*Altern Ther Health Med.* 2023;29(3):240-245).

Weidong Jia, Mmed; Liangkui Wei, Mmed; Jianfeng Li, Mmed; Bing Xia, PhD; Weiming Hu, Mmed; Yu Zhang, Mmed; Fuyun Liu, PhD; Department of Pediatric Orthopedics, The Third Affiliated Hospital of Zhengzhou University, Zhengzhou, China. **Xianxu Zeng, PhD;** Department of Pathology, The Third Affiliated Hospital of Zhengzhou University, Zhengzhou, China.

Corresponding author: Fuyun Liu, PhD
E-mail: liufuyun111@126.com

INTRODUCTION

Tight filum terminale syndrome (TFTS) refers to cases in which the filum terminale (FT) is infiltrated by adipose tissue or undergoes fibrous degeneration, pulls on the conus medullaris (CM), and restricts the retraction of the spinal cord, causing ischemia and hypoxia that disrupt oxidative metabolism in the nerve cells of the spinal cord, leading to neural injury.[1,2]

TFTS is a stretch-induced functional disorder of the spinal cord, resulting in progressive motor and sensory abnormalities of the lower extremities, scoliosis and/or urinary dysfunction and lumbar and dorsal hirsutism.[3,4] Magnetic resonance imaging (MRI) of the spinal cord in most children can find structural changes such as thickening of the FT, steatosis or low position of the CM.[5]

However, some children with TFTS have apparent clinical symptoms, but a normal MRI,[6-8] so that diagnosing TFTS before making an FT histopathological examination (HPE) is significantly difficult. Once a child develops neurological dysfunction, most patients benefit a little from undergoing surgery. As early treatment, prophylactic surgery is safe and effective in preventing neurological deficits.[9]

Optical coherence tomography (OCT) is a rapid optical imaging technique that does not damage the tissue and has been used in ophthalmology and oncology.[10,11] OCT can perform an "optical biopsy" by observing changes to the inner microstructure of tissues *in vivo*.[12]

In this study of OCT-based *ex vivo* specimens, we conducted a pilot project and *ex vivo* examination of FTs, and determined the high sensitivity and accuracy of OCT in the diagnosis of TFTS, revealing the advantages of OCT imaging in the diagnosis of FT lesions.

Table 1. Clinical Manifestation in the 12 Children with TFTS

#	Age	Gender	Conus Medullaris Position	Residual urine in bladder	Hydronephrosis	Abnormal stool	Abnormal urination	Lower limb deformity
1	1 month	female	L3	no	no	√	no	no
2	8 years	female	L1	no	no	√	√	√
3	1 month	female	L3	no	no	√	no	no
4	2 months	male	L2	6 ml	√	no	no	√
5	3 months	male	L2	no	no	no	no	no
6	3 months	male	L4	22 ml	no	√	no	no
7	3 years	female	L3	no	no	√	no	√
8	1 year	female	L1	13 ml	no	√	no	no
9	5 months	male	L1	19 ml	no	√	no	no
10	3 years	male	L1	no	no	√	no	no
11	3 months	male	L4	51 ml	no	no	no	√
12	2 months	male	L1	17 ml	√	no	no	no

MATERIALS AND METHODS

General Information

In our study, FTs from 32 children diagnosed with TFTS were collected from the Department of Spine and Spinal Cord from October 2020 to September 2021. According to the screening criteria, we selected 12 cases (Table 1), including 7 males and 5 females, age range 1 month to 8 years with an average age of 1.4 years. Diagnosis of TFTS was based on clinical presentation, physical and radiological examinations, ultrasound of the kidney and bladder and MRI.

The study was submitted to the hospital ethics committee for approval, and informed consent of family members was obtained.

Inclusion criteria. Cases with: (1) spinal cord MRI showing a normal or abnormal FT; (2) normal CM position or below the lower edge of lumbar 2 (L2); (3) lower limb deformity, sensorimotor dysfunction or defecation dysfunction.

Exclusion criteria. Cases with (1) low position and tethering of the CM caused by split cord malformation; (2) spinal cord neural injury caused by compression of lipoma inside and outside the spinal canal; (3) spinal cord nerve root adhesion after spinal canal operation; (4) tethered cord syndrome caused by congenital meningocele and valgus deformity.

We collected 2 fetuses, age 28 and 35 weeks with non-spinal nervous system disease that had been aborted in our hospital. Both fetuses had flat lumbosacral skin without pigmentation or abnormal hair. After confirming that they had normal spinal cords, their FTs were sent for HPE and OCT scanning.

Surgery and Experiment

In the TFTS group, the FTs were removed by the same group of doctors. Intraoperative electrophysiological monitoring was performed, and at least 2 cm of the FT was removed under a microscope. In the TFTS group (Figure 1A, 1B, 1C), the FTs were light red or pale regardless of whether CM was in the correct position at L2 or below L2. A total of 7 children's FT were ≥2.2 mm in diameter and exhibited various characteristics. Some FTs were shortened and thickened, some had uniform thickness, some had expansion mostly at one end and some had an irregular form. In terms of color, some FTs were light yellow, some were white and red. In the other 5 children in the TFTS group, their FTs were 1.1 to 2.0 mm in diameter with low elasticity and high strain and were attached in a bow-like manner to the posterior wall of the spinal canal; they were light red or pale. One (1/5) child's CM was in the correct position, and the MRI findings were normal (Figure 1D); 4 (4/5) children had lower CM, and their MRI findings were abnormal.

Figure 1. The diseased FT in surgery and the MRI of the diseased FT. (**1A**) The diseased FT in the TFTS group was inelastic, a light pale color and attached in a bow-like manner to the posterior wall of the spinal canal; (**1B**, **1C**) The diseased FTs were >1.8 mm in diameter and exhibited fibrous tissue hyperplasia. The FTs had various characteristics; most had vascular structure proliferation and were redder in color; (1D) the MRI images of some children with TFTS show the position of CM was standard at the L2 level (indicated by the arrow).

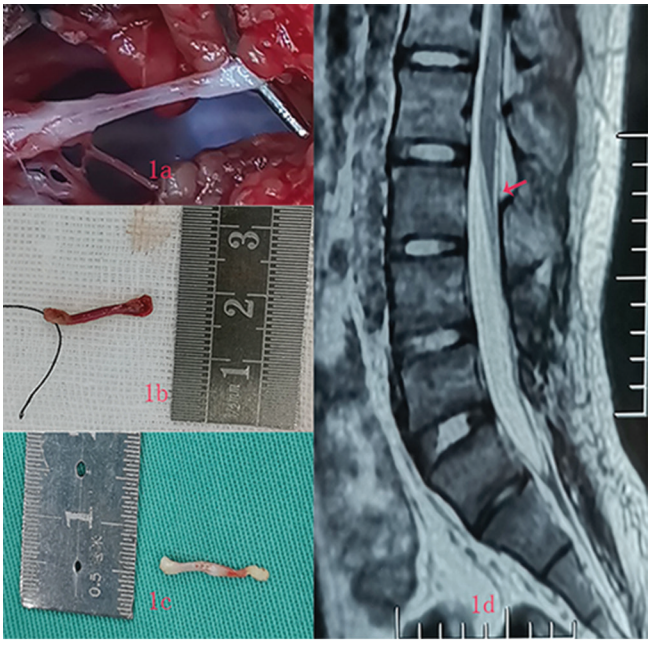

Abbreviations: FT, filum terminale; CM, conus medullaris; MRI, magnetic resonance imaging; TFTS, tight filum terminale syndrome.

Figure 2. HPE and OCT images of the diseased FT. (**2A**) Under a microscope (H&E staining; original magnification, 10^{20}), the surface of the FT consisted of fibrous tissue (long arrow) with thickened and irregular morphology, while the interior of the FT contained many adipocytes (short arrow) and was vacuolar- and grid-like; (**2B**) Dense fibrous bundles (long arrow) were seen on the surface of the FT with strong shading in the OCT images, while the adipose tissue inside the FT (short arrow) had weaker refraction than the fibrous tissue.

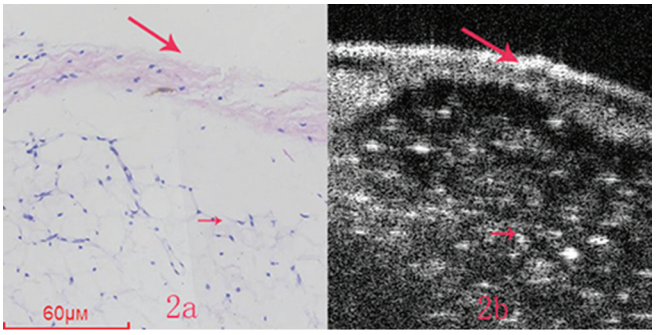

In the fetal group, FTs were cut from the end of the CM below the 12th vertebral body, which allowed us to see whether or not the CM corresponded to the correct position of the vertebral body, the lower edge of L2. In the 2 fetuses, the FTs were approximately 0.8 to 1.6 mm, of uniform diameter, and highly elastic with a little pale or red color; the CM was located above the L2 edge.

After cutting the FTs, they were transferred to test tubes and subjected to OCT scanning (axial resolution ≤5 μm, lateral resolution ≤10 μm). After obtaining the OCT images and marking the scanning sites, the FTs were soaked in neutral buffered 10% formalin solution and then subjected to HPE for microscopic imaging. OCT images were precisely compared with the corresponding histological images.

Statistical Analysis

Statistical analysis was performed using IBM™ SPSS 22.0 software, and 2 assessors performed blinded qualitative analysis of the OCT images. The results were compared via Chi-square test (McNemar test) and receiver operating characteristic (ROC) curve. $P \leq .05$ was considered statistically significant.

RESULTS

The Morphology of FTs in the Fetal and TFTS Groups via HPE and OCT

TFTS group. Under a microscope, adipose infiltration and capillary increase were significantly greater than in the fetal group (Figures 2 to 4). Many FTs showed obvious fibroplasia and disarrangement along with hyaline degeneration, and some scattered nerve cells were observed. OCT images showed significantly increased adipose tissue in which the adipocytes were arranged in a grid-like pattern. FTs had dense and disordered fibrous tissue, in which vascular-like tissue could be seen, along with occasional nerve cells.

Figure 3. HPE and OCT images of the vascular structures of diseased FT (H&E staining; original magnification, 10^{20}). (**3A**) Under a microscope, the diseased FT showed hyperplastic and disordered fibrous tissue and increased vascular structures (arrow); (**3B**) OCT showed the vascular structure, weak refraction.

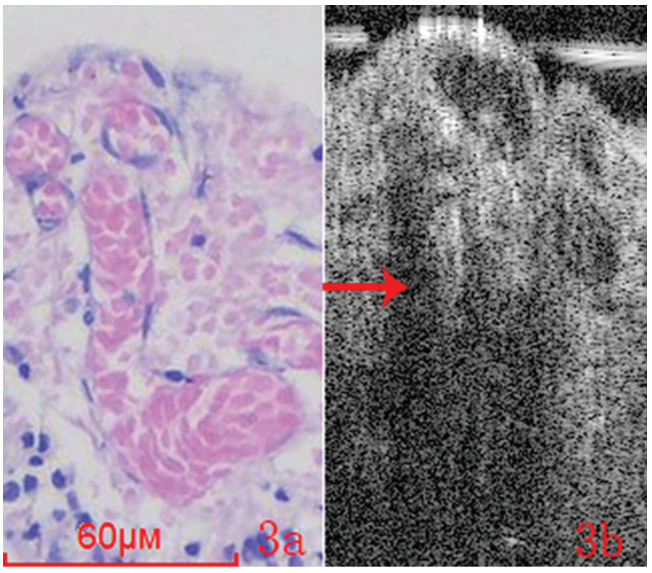

Figure 4. The HPE and OCT images of fibrous tissues in diseased FTs with H&E staining; original magnification, (10^{20}). (**4A**) Under a microscope, the fibrous tissues were hyperplastic and disordered, thickened and distorted and were adhered or fused to different degrees (long arrow); (**4B**) OCT showed elastic fibers were irregular, dense and with varying degrees of proliferation, and showed different refractivity with the interstitial spaces appearing as light-colored strips of weak refraction (short arrow).

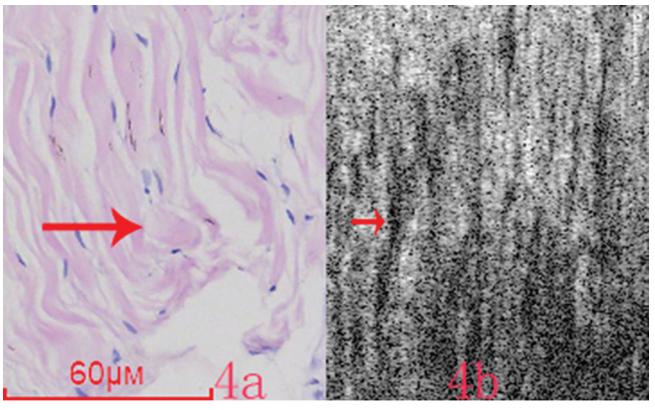

Fetal group. Under a microscope, we could see a large amount of loose connective tissue composed of longitudinally oriented fibrous tissue scattered with capillaries but no adipose tissue (Figure 5). The OCT showed the fiber bundles with strong refraction in the FTs; between the fiber bundles there was weak refraction of the interstitial space.

Figure 5. Image of FT from the fetal group by HPE (H&E staining, original magnification, 10^{20}). Under a microscope, a large amount of loose connective tissue was seen (arrow), composed of longitudinally oriented fibrous tissue cells interspersed with capillaries but no adipose tissue. Compared with the TFTS group (**Figure 2A**), fibrous tissue of the diseased FT was thickened and had irregular morphology (long arrow), and the interior of the FT contained many adipocytes (short arrow).

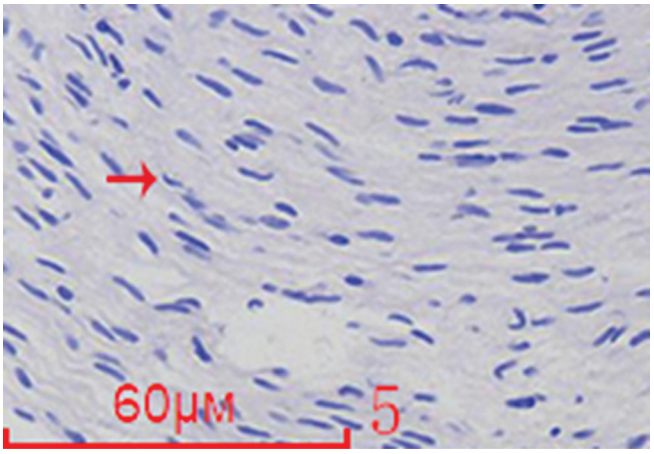

Figure 6. The ROC curve of MRI and OCT; AUC was 0.966 with OCT and 0.649 with MRI.

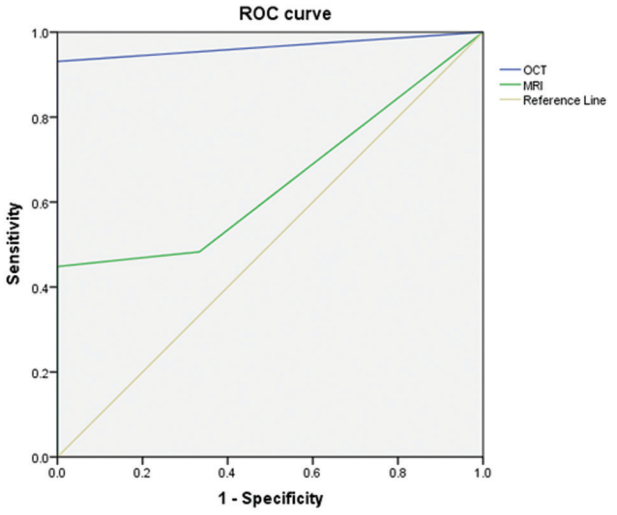

Table 2. Diagnostic Results of the 14 FT Samples

Number	Filum Terminal (width×height×length)	MRI Diagnosis	Histopathological Examination	OCT Diagnosis 1	OCT Diagnosis 2
TFTS 1	3mm×1mm×2 cm	+	+	+	+
TFTS 2	4mm×1mm×2 cm	-	+	+	+
TFTS 3	2mm×2mm×2 cm	+	+	-	-
TFTS 4	1.2mm×1mm×3 cm	±	-	-	-
TFTS 5	1mm×1mm×2 cm	±	+	-	-
TFTS 6	6mm×2mm×3 mm	+	+	+	+
TFTS 7	2mm×1mm×2 cm	+	+	+	+
TFTS 8	3mm×1mm×3 cm	-	+	+	+
TFTS 9	1.8mm×1mm×2 cm	-	+	+	+
TFTS10	2.2mm×2mm×3 cm	-	+	+	+
TFTS11	8mm×2mm×13 cm	+	+	+	+
TFTS12	3mm×2mm×2 cm	-	+	+	+
Fetus 1	0.8mm×0.5mm×1cm	-	-	-	-
Fetus 2	1.6mm×1mm×2cm	-	-	-	-

Abbreviations: -, position of conus medullaris (CM) is above the upper edge of lumbar 2 level (L2).; **±,** position CM ranges from upper edge to the lower edge of L2; +, position of CM is below the lower edge of L2.

Comparison of HPE and OCT Results

The diagnostic results of the 14 FT samples are shown in Table 2. Our CT and HPE diagnostic results were consistent (Kappa = 0.659; $P = .009$, <.01). There was no statistically significant difference between OCT and HPE in diagnosing TFTS using a Chi-square test (McNemar test; $P \geq .5$). Positive results were 11/14 (78.6%) by HPE, and the positive HPE rate was higher than the OCT rate in 9/14 children (64.3%) because 2 children in the TFTS group were positive by HPE but negative by OCT (false negative). The statistical result proved that the accuracy and sensitivity of diagnosing TFTS with OCT were similar to with HPE.

OCT and MRI ROC Curve and Area Under the Curve (AUC)

We took HPE as the gold standard in diagnosing TFTS and drew the MRI and OCT curves (Figure 6; IBM™ SPSS software version 21). We observed that the OCT AUC (AUG = 0.966; 95% CI, 0.903 to 1.000) was better than with MRI (AUG = 0.649; 95% CI, 0.403 to 0.896), which suggested that the sensitivity and specificity of OCT were better than MRI. We also focused on the positive rate with MRI: for all samples, 50% (7/14) patients were positive with MRI and lower than with OCT (9/14; 64.3%). In our study, the sensitivity and specificity of diagnosing TFTS with OCT were better than with MRI.

DISCUSSION

Study of Normal FTs

The FT extends from the end of the CM to the end of the spinal canal, divided into 2 parts by the dural sac. A normal FT provides the proper elasticity to protect the spinal cord against mechanical stress.[13] Filippidis, et al.[1] suggested that the traction of CM and FT triggers a complex cascading cell and molecule reaction, leading to ischemia and hypoxia at the end of the spinal cord, abnormal metabolism, changes in the structure of the distal spinal cord and clinical manifestations of tethered cord syndrome.We defined significantly fatty infiltration and fibroplasia as the criteria to distinguish normal and diseased FTs. We found that the average FT diameter in the fetal group (28 weeks and 35 weeks) was 1.2 mm (0.8 mm to 1.6 mm), and the position of the CM was above the L2 edge. Under a microscope, the FT was mainly composed of uniformly arranged fibrous tissue and capillaries. Pinto, et al.[14] observed the FTs in 20 normal adults by light microscopy and scanning electron microscopy. They found that the FTs were mainly composed of longitudinally arranged collagen fibers, which verified our study findings.

Study of Diseased FTs and TFTS

We studied the TFTS group's FTs and found disordered elastic fibers, prominent adipose infiltration and significantly increased capillaries. We could distinguish the disarrangement of structural characteristics between the diseased and normal FTs. Through animal experiments, Yamada, et al.[15] found that when the diseased FT stretches the CM, no matter the position of the CM, it will cause ischemia and hypoxia, leading to changes in cellular metabolism in the spinal cord and subsequent nerve injury. They found adipose infiltration and collagen proliferation in the FTs by light microscopy and electron microscopy. Thompson, et al.[5] suggested that all diseased FTs have noticeable fibrous changes. Barutcuoglu, et al.[3] found that abnormal FTs with a normal outward appearance may, upon closer inspection, present with dense collagen fibers, vast and numerous capillaries and hyaline membrane formation. In contrast, normal FTs are a mixture of collagen fibers and blood vessels in which the elastic fibers disappear. By scanning electron microscopy, Liu, et al.[16] observed diseased FTs with TFTS. They found abundant collagen bundles and adipocytes, disordered elastic fibers and reticular fibers in the FTs by observing the ultrastructure.

Applying OCT in Diagnosing TFTS.

The most accurate and reliable method for diagnosing TFTS is HPE, which requires biopsy or surgery, causing some tissue damage. OCT is a significant breakthrough after ultrasound, X-ray, CT and MRI. OCT imaging makes no contact with the skin and is entirely non-invasive, and can provide real-time 2- and 3-dimensional images with micron resolution at a tissue depth of several millimeters.[17,18] OCT resolution is close to that of HPE, and can significantly distinguish between the internal structural characteristics of diseased and normal tissue. In our study, we used OCT for scanning the FT of normal fetuses and children with TFTS and were able to observe the inner FT structure and distinguish the differences between normal and diseased FTs. Some of the OCT images were highly consistent with the pathological examination, and the sensitivity and accuracy of OCT in the diagnosis of TFTS were high. However, we also found some shortcomings, such as difficulty observing nerve cells under OCT, which we considered the result of limited technical operation.

TFTS is a controversial topic in pediatric neurosurgery in terms of diagnosis, clinical manifestations and treatment. Investigation and treatment is solely based on clinical criteria, unlike other occult malformations, as patients may not exhibit any skin stigmata.[19] The first description of this syndrome is based on radiological images of a low-lying spinal cord indicating evidence of spinal dysraphism or at least a thickened FT. However, radiological abnormalities are no longer required for diagnosis.[20] Diagnosis based on radiological images, especially as an incidental finding without clinical evidence, may lead to over-treatment with unnecessary surgical interventions.[21] We aim to detect these FTs via OCT and confirm the diagnosis with clinical symptoms to be able to seek suitable surgical indications and avoid unnecessary surgical cutting of the FT.

In this study, the accuracy of diagnosing TFTS by OCT was high; we still need more FT samples for this study because 2 children (2/12) in the TFTS group were false negative. Our research confirmed that OCT can clearly show the inner structure of FT, but there is no instrument for preoperative examination, and FT can only be studied *in vitro*. Okay, et al.[22] used a nasal speculum and the transsphenoidal approach during the endoscopic surgical procedure of untethering FTs. Endoscopic release of an FT is a safe technique, especially if it is performed with neuromonitoring; it may shorten hospital stays and reduce perioperative blood loss. We plan to use an endoscope combined with an OCT instrument to get the inner structure of FTs *in vivo*; endoscopic release of an FT may be a better choice once it is found to be diseased. Using an endoscope plus OCT will make it easy to diagnose TFTS and untether an FT.

CONCLUSION

OCT can quickly obtain clear images of the inner structure of FT, can contribute to diagnosing TFTS, and will be an indispensable complement to MRI and HPE. More studies of FT samples *in vivo* are needed to confirm the high accuracy rate of OCT.

ETHICS APPROVAL

Ethics approval was obtained from the Ethics Committee of the Third Affiliated Hospital of Zhengzhou University (2019.NO.74)

CONFLICT OF INTEREST

None.

AUTHOR CONTRIBUTIONS

Weidong Jia, Liangkui Wei, and Jianfeng Li contributed equally to this work.

REFERENCES

1. Filippidis AS, Kalani MY, Theodore N, Rekate HL. Spinal cord traction, vascular compromise, hypoxia, and metabolic derangements in the pathophysiology of tethered cord syndrome. *Neurosurg Focus*. 2010;29(1):E9. doi:10.3171/2010.3.FOCUS1085
2. Yamada S, Knerium DS, Mandybur GM, Schultz RL, Yamada BS. Pathophysiology of tethered cord syndrome and other complex factors. *Neurol Res*. 2004;26(7):722-726. doi:10.1179/016164104225018027
3. Barutcuoglu M, Selcuki M, Selcuki D, et al. Cutting filum terminale is very important in split cord malformation cases to achieve total release. *Childs Nerv Syst*. 2015;31(3):425-432. doi:10.1007/s00381-014-2586-1
4. Hertzler DA II, DePowell JJ, Stevenson CB, Mangano FT. Tethered cord syndrome: a review of the literature from embryology to adult presentation. *Neurosurg Focus*. 2010;29(1):E1. doi:10.3171/2010.3.FOCUS1079
5. Thompson EM, Strong MJ, Warren G, Woltjer RL, Selden NR. Clinical significance of imaging and histological characteristics of filum terminale in tethered cord syndrome. *J Neurosurg Pediatr*. 2014;13(3):255-259. doi:10.3171/2013.12.PEDS13370
6. Bao N, Chen ZH, Gu S, Chen QM, Jin HM, Shi CR. Tight filum terminale syndrome in children: analysis based on positioning of the conus and absence or presence of lumbosacral lipoma. *Childs Nerv Syst*. 2007;23(10):1129-1134. doi:10.1007/s00381-007-0376-8
7. Tubbs RS, Oakes WJ. Can the conus medullaris in normal position be tethered? *Neurol Res*. 2004;26(7):727-731. doi:10.1179/016164104225017910
8. Warder DE, Oakes WJ. Tethered cord syndrome: the low-lying and normally positioned conus. *Neurosurgery*. 1994;34(4):597-600. doi:10.1227/00006123-199404000-00005
9. Kasliwal MK, Mahapatra AK. Surgery for spinal cord lipomas. *Indian J Pediatr*. 2007;74(4):357-362. doi:10.1007/s12098-007-0060-8
10. Hariri LP, Bonnema GT, Schmidt K, et al. Laparoscopic optical coherence tomography imaging of human ovarian cancer. *Gynecol Oncol*. 2009;114(2):188-194. doi:10.1016/j.ygyno.2009.05.014
11. Titiyal JS, Kaur M, Nair S, Sharma N. Intraoperative optical coherence tomography in anterior segment surgery. *Surv Ophthalmol*. 2021;66(2):308-326. doi:10.1016/j.survophthal.2020.07.001
12. Fujimoto JG, Pitris C, Boppart SA, Brezinski ME. Optical coherence tomography: an emerging technology for biomedical imaging and optical biopsy. *Neoplasia*. 2000;2(1-2):9-25. doi:10.1038/sj.neo.7900071
13. De Vloo P, Monea AG, Sciot R, van Loon J, Van Calenbergh F. The Filum terminale: A cadaver study of anatomy, histology, and elastic properties. *World Neurosurg*. 2016;90:565-573.e1. doi:10.1016/j.wneu.2015.12.103
14. Pinto FC, Fontes RB, Leonhardt C Mde, Amodio DT, Porro FF, Machado J. Anatomic study of the filum terminale and its correlations with the tethered cord syndrome. *Neurosurgery*. 2002;51(3):725-729; 729-730.
15. Yamada S, Won DJ, Pezeshkpour G, et al. Pathophysiology of tethered cord syndrome and similar complex disorders. *Neurosurg Focus*. 2007;23(2):E6. doi:10.3171/FOC-07/08/E6
16. Liu FY, Li JF, Guan X, Luo XF, Wang ZL, Dang QH. SEM study on filum terminale with tethered cord syndrome. *Childs Nerv Syst*. 2011;27(12):2141-2144. doi:10.1007/s00381-011-1414-0
17. He Z, Wang P, Ye X. Novel endoscopic optical diagnostic technologies in medical trial research: recent advancements and future prospects. *Biomed Eng Online*. 2021;20(1):5. doi:10.1186/s12938-020-00845-5
18. Zhou C, Alex A, Rasakanthan J, Ma Y. Space-division multiplexing optical coherence tomography. *Opt Express*. 2013;21(16):19219-19227. doi:10.1364/OE.21.019219
19. Komagata M, Endo K, Nishiyama M, Ikegami H, Imakiire A. Management of tight filum terminale. *Minim Invasive Neurosurg*. 2004;47(1):49-53. doi:10.1055/s-2003-812463
20. Drake JM. Occult tethered cord syndrome: not an indication for surgery. *J Neurosurg*. 2006;104(5)(suppl):305-308.
21. Drake JM. Surgical management of the tethered spinal cord--walking the fine line. *Neurosurg Focus*. 2007;23(2):E4. doi:10.3171/FOC-07/08/E4
22. Okay O, Dalgic A, Yildirim AE, et al. Endoscopic untethering of tight filum terminale: an operative technique. *Turk Neurosurg*. 2021;31(1):73-75.